Electron-phonon interaction in C_{70}

D. Provasi
Dipartimento di Fisica, Università di Milano, Via Celoria 16, I-20133 Milano, Italy

N. Breda
Dipartimento di Fisica, Università di Milano, Via Celoria 16, I-20133 Milano, Italy
and INFM, Sezione di Milano, Via Celoria 16, I-20133 Milano, Italy

R. A. Broglia
Dipartimento di Fisica, Università di Milano, Via Celoria 16, I-20133 Milano, Italy
INFN, Sezione di Milano, Via Celoria 16, I-20133 Milano, Italy
and The Niels Bohr Institute, University of Copenhagen, D-2100 Copenhagen, Denmark

G. Colò
Dipartimento di Fisica, Università di Milano, Via Celoria 16, I-20133 Milano, Italy
and INFN, Sezione di Milano, Via Celoria 16, I-20133 Milano, Italy

H. E. Roman
INFN, Sezione di Milano, Via Celoria 16, I-20133 Milano, Italy

G. Onida
Istituto Nazionale per la Fisica della Materia, Dipartimento di Fisica dell'Università di Roma Tor Vergata, Via della Ricerca Scientifica, I-00133 Roma, Italy

(Received 6 May 1999)

The matrix elements of the deformation potential of C_{70} are calculated by means of a simple, yet accurate solution of the electron-phonon coupling problem in fullerenes, based on a parametrization of the ground-state electronic density of the system in terms of sp^{2+x} hybridized orbitals. The value of the calculated dimensionless total electron-phonon coupling constant is $\lambda \approx 0.1$, an order of magnitude smaller than in C_{60}, consistent with the lack of a superconducting phase transition in $C_{70}A_3$ fullerite, and in overall agreement with measurements of the broadening of Raman peaks in $C_{70}K_4$. We also calculate the photoemission cross section of C_{70}^-, which is found to display less structure than that associated with C_{60}^-, in overall agreement with the experimental findings.

I. INTRODUCTION

The discovery that some alkali-doped C_{60} compounds are superconducting[1–5] with a transition temperature as high as 40 K for the fulleride $C_{60}Cs_3$ under pressure[6] has triggered considerable interest in the study of fulleride doped materials at low temperatures. Much effort has been concentrated in trying to understand whether such large values of T_c can be caused by the coupling of electrons to phonons. The electron-phonon coupling constants for C_{60} have been estimated both from experiments[7] and calculations.[8] There exists some consensus on the fact that C_{60} compounds are *s*-wave BCS-like superconductors driven by the coupling to selected intramolecular phonons.[8] On the other hand, no calculation of this coupling exists in the literature for the case of C_{70}. Since the associated alkali compounds display no superconductivity, with a smooth and continuous behavior of the resistivity down to about 1 K,[9] it is an important issue to compare the electron-phonon coupling constant for C_{70} with that of C_{60}.

In the present paper we address this problem from a theoretical point of view, computing the deformation potential of C_{70} and extracting the associated total electron-phonon coupling constant, λ. It will be concluded that the resulting value of λ is much smaller than in C_{60}, essentially ruling out the possibility of a superconducting phase at low temperatures for doped fullerides built out of C_{70}.

This negative result, which can be understood in rather general, qualitative structural terms, as discussed at the end of Sec. II, has two positive oucomes: first, it provides further evidence for the *s*-wave BCS-like mechanism at the basis of alkali-doped fullerides superconductivity. Second, it sheds light on the properties fullerenes have to exhibit to be ''good'' building blocks of eventual organic superconductors, indicating the direction of the highly symmetric, small fullerenes (cf. also Refs. 10 and 11), a strategy which seems to be universally valid also for other compact systems, like the atomic nucleus.[12]

In the production of fullerene clusters by means of laser vaporization or arc discharge the yield of C_{70} can be optimized, by varying the experimental conditions,[13,14] up to a ratio of about 10% of C_{70} with respect to C_{60}. This allows the production of sufficiently large amounts of C_{70} for the synthesis of C_{70} molecular crystals.[15] Hence the structural

and electronic properties of C_{70} can be experimentally studied, and compared with those of C_{60}. In analogy with the case of solid C_{60}, C_{70} crystals can be doped with alkali metals, and the conductivity of the resulting compounds can be investigated.

On the theoretical side, *ab initio* methods based on the local-density approximation (LDA) (Ref. 16) have been applied to the study of the ground-state properties of C_{70}. The ionic configuration, characterized by a D_{5h} geometry, is consistent with the NMR measurements,[17] and the electronic structure agrees reasonably well with ultraviolet photoemission spectroscopy (UPS) data. We adopt in this work the ground-state geometry of Ref. 16. The vibrational properties of C_{70} have been studied in Ref. 18, starting with the same geometry. A simplified model like the bond charge model (BCM) is nevertheless able to reproduce the experimental values for the optically active frequencies within 4%.[19] Indeed, beyond the electronic and vibrational properties, *ab initio* methods also allow us to compute the coupling between these two degrees of freedom without the need of introducing any adjustable parameter. However, *ab initio* methods in the case of large clusters, such as C_{60} and C_{70}, are computationally demanding and may not be particularly transparent. As an alternative, in order to extract the electron-phonon coupling constants, it is possible to adopt a simplified numerical method which already proved to be satisfactory in the case of C_{60}.[20] This method, albeit approximated, has been shown to lead to quite satisfactory results, also because it is devised to take into account accurate phonon eigenvectors, which are known to influence very strongly the matrix elements of the deformation potential. In fact, the relative strength of the latter is strictly related to the bond stretching associated to the ionic displacements. In the present work, using the scheme introduced in Ref. 20 for C_{60}, we address the case of C_{70}.

II. ELECTRON-PHONON COUPLING

Our calculation starts with the determination of the electronic states of fullerene-C_{70}, and the corresponding electron density, within LDA. We include the exchange and correlation effects according to the parametrization of Perdew and Zunger[21] of the Monte-Carlo results of Ceperley and Alder.[22] No generalized gradient approximation (GGA) corrections are considered, since LDA is known to yield very accurate results for the equilibrium geometry and charge density in such covalently bonded carbon systems.[23] The role of carbon atoms is taken into account using *ab initio* norm-conserving pseudopotentials.[24] A spherical basis, made up with states which are solution of a central potential which mimics the $L=0$ component of the LDA local potential, is employed. Spherical wave functions with n and l respectively up to 15 and 20 are included in the basis (this gives ≈ 4000 basis vectors). The Kohn-Sham equations are solved in matrix form on this basis, as described in more detail in Ref. 25. In that work the maximum values of n and l were slightly different, but the results are essentially the same. The highest occupied-lowest unoccupied molecular orbital (HOMO-LUMO) gap is 1.87 eV, in agreement with other LDA calculations.[16] As in C_{60}, errors due to the neglect of both self-energy and excitonic effects nearly cancel each other, leading to a theoretical value close to the experimentally measured optical gap (1.6 ± 0.2 eV). The Kohn-Sham levels up to about -10 eV are in overall agreement with the UPS spectra. The symmetries of the HOMO and LUMO levels (E_1'') are the same as those obtained in Ref. 16. The different results of Ref. 26 are probably an artifact due to the limited basis set used there.

The energies and eigenvectors of the vibrational normal modes have been taken from a BCM calculation.[27] Then, following Ref. 20, we have parametrized the *ab initio* electronic density in terms of sp^{2+x} hybrid orbitals obtained as linear combinations of the four s and p valence orbitals of each carbon atom. Three of the hybrid orbitals are directed along the bonds connecting the atom with its three nearest neighbors, while the fourth is determined by orthogonality conditions and takes care of the additional π bonding present in the fullerenic cages. The radial wave functions of the s and p orbitals are taken as simplified Slater wave functions [$R_s = (2/\sqrt{\sigma_1^3}) e^{(-r/\sigma_1)}$ and $R_p = (2/\sqrt{3\sigma_2^5}) r e^{(-r/\sigma_2)}$], where the parameters σ_1 and σ_2 have been adjusted in order to obtain the best fit to the C_{70} charge density computed in LDA. This leads to $\sigma_1 = 0.66$ Å and $\sigma_2 = 0.36$ Å [to be compared with similar values obtained in the case of C_{60} (Ref. 20)].

After having determined the hybrid orbitals, we can write the contribution to the total electronic density arising from a single atom, and carry out a multipole expansion of it around the center of the cluster. Adding the contributions of the 70 atoms one obtains the total density. The deformation potential associated with a normal mode α is then

$$V_{def}^{(\alpha)}(\vec{r}) = \sum_{N=1}^{70} \vec{Q}_N^{(\alpha)} \cdot \vec{\nabla}_N V_{TOT}(\vec{r}, \{\vec{R}\})|_{\{\vec{R}\}=\{\vec{R}^0\}}, \qquad (1)$$

where $\vec{Q}_N^{(\alpha)}$ is the displacement of the Nth ion, V_{TOT} is the total LDA electronic potential, and $\{\vec{R}\}$ represents the whole set of ionic coordinates whose equilibrium values are $\{\vec{R}^0\}$ ($\vec{Q}_N = \vec{R}_N - \vec{R}_N^0$). The pseudopotential term of V_{TOT} displays an explicit dependence on the ionic positions, therefore the calculation of its gradient presents no difficulties. On the other hand, the Hartree and exchange-correlation (XC) terms depend on $\{\vec{R}\}$ *implicitly* through the electronic density ϱ. We thus write

$$\sum_N \vec{Q}_N \cdot \vec{\nabla}_N V_{\text{Hartree},XC}[\varrho(\vec{r}, \{\vec{R}\})] = \sum_N \frac{\partial V_{\text{Hartree},XC}[\varrho]}{\partial \varrho} \vec{Q}_N \cdot \vec{\nabla}_N \varrho(\vec{r}, \{\vec{R}\}). \qquad (2)$$

While one can easily calculate $\partial V / \partial \varrho$, the gradient of the total density is determined by assuming, within the present hybrid orbital model, that upon moving the ions according to the phonon eigenvectors the hybrid orbitals change their direction but *not* their shape. This makes the calculation quite simple and transparent, since it is possible to visualize the effect of a normal ionic displacement on the electronic orbitals. Finally, we can evaluate the matrix elements of the deformation potential, $[V_{def}^{(\alpha)}]_{ij} \equiv \langle i | V_{def}^{(\alpha)} | j \rangle$, between Kohn-Sham wave functions.

TABLE I. Reduced electron-phonon matrix element g_α and partial coupling constants $\lambda_\alpha/N(0)$ for the LUMO electron state and selected phonons of C_{70}. The first two columns report the calculated phonon frequencies and symmetries obtained within a bond-charge model calculation (Ref. 27). In the fifth column we also show the calculated widths of the phonon peaks [Eq. (4)]. For comparison, the last two columns give the experimental frequencies and the measured widening γ of the Raman peaks in going from pure C_{70} to K_4C_{70} films.

Theory					Experiment (Ref. 29)	
Frequency [cm^{-1}]	symm.	g_α [meV]	$\lambda_\alpha/N(0)$ [meV]	γ[cm^{-1}]	Frequency[cm^{-1}]	γ[cm^{-1}]
230	E_2'	4.77	0.798	2.36	226	10.7
271	A_1'	21.9	7.136	58.7	256	−1.5
308	E_2'	6.03	0.951	5.06		
425	A_1'	3.59	0.122	2.48	394	6.3
442	E_2'	3.76	0.258	2.82	408	−0.5
448	A_1'	4.95	0.220	4.96	454	4.9
508	E_2'	3.26	0.169	2.44		
590	E_2'	3.09	0.130	2.55		
625	A_1'	1.95	0.025	1.08	567	3.5
701	A_1'	1.71	0.017	0.93	702	13.9
736	E_2'	6.98	0.533	16.2	712	14.3
764	E_2'	2.48	0.065	2.12	737	0.5
1089	E_2'	2.66	0.052	3.48		
1200	A_1'	1.73	0.010	1.62	1181	12.9
1223	A_1'	1.46	0.007	1.18	1228	6.5
1368	A_1'	6.45	0.123	25.7	1444	9.0
1459	A_1'	6.79	0.127	30.4	1459	

If one is interested in the behavior of the conductivity in alkali-doped fullerites, or in the photoemission spectrum of C_{70}, we should start from phonon energies, and deformation potentials, evaluated by using the electronic density of a negative charged ion. On the other hand, because the density of the 280 valence electrons of C_{70} is not appreciably altered by adding a few more electrons, one expects the matrix elements of the deformation potentials associated with C_{70} and with $C_{70}^{n-}(1\leqslant n\leqslant 4)$, to be rather similar.

We evaluate, for each phonon α, the *reduced* matrix elements $[V_{def}^{(\alpha)}]_{ii}$ (corresponding to a given electronic state i) which are denoted by g_α, as well as the partial electron-phonon coupling constants λ_α defined as

$$\lambda_\alpha/N(0)=Cg_\alpha^2/\hbar\omega_\alpha. \tag{3}$$

In the above expression, $N(0)$ is the density of levels at the Fermi energy, ω_α are the phonon frequencies, and C is $d_\alpha/2$,d_α being the degeneracy of the phonon state.[28] The results corresponding to the LUMO (E_1'') and the A_1' and E_2' phonons, are collected in Table I. We only report those phonons yielding a non-negligible partial coupling, i.e., $\lambda_\alpha/N(0)\geqslant 0.005$ meV. For these phonons, we also show the value of the full width at half maximum (FWHM) of the Raman peaks (γ_α), due to the decay into electron-hole pairs, widths which are connected to the partial couplings by the relation[8]

$$\gamma_\alpha=\frac{2\pi\omega_\alpha^2 N(0)\lambda_\alpha}{d_\alpha}. \tag{4}$$

These widths show up as additional broadenings of the Raman peaks when the LUMO electronic state becomes occupied, e.g., in the case of K_4C_{70}. The differences between the widths of the Raman peaks of K_4C_{70} and those of the peaks of bare C_{70} films have been measured,[29] and are reported in the last column of Table I. However, a direct comparison with the theoretical results displayed in the fifth column of Table I is not straightforward for several reasons. First of all, it must be observed that subtracting the phonon widths measured in pure C_{70} from that measured in K_4C_{70} leads, in some cases, to unrealistic negative values. Then, one should be aware of the fact that the frequencies and symmetry assignements of the experimental peaks are affected by some uncertainty. In any case, we followed the assignements given in Refs. 30 and 19, which are different from those of Ref. 29, since the former refer to low-temperature, higher resolution spectra, and rely also on calculations of the phonon peaks strength.[31] Finally, the value of $N(0)$ is not known with precision: we assume a value of 12 eV^{-1} as suggested by Ref. 29, but any value within the range 6–30 eV^{-1} seems to be equally possible.[8] The total electron-phonon coupling constant λ (sum of the partial coupling constants) computed making use of the results reported in the fifth column of Table I, and of the empirical values of γ_α (seventh column of Table I), are quite similar and of the order of 0.1. Keeping in mind the above-mentioned caveats, we may hence speak of an overall agreement between the results of the present calculation and the experimental findings. If $N(0)$ varies between 6 and 30 eV^{-1}, the theoretical total coupling constant varies between 0.05 and 0.25. These values must be compared with a value essentially equal to 1 obtained in the case of C_{60} (cf., e.g., Refs. 8 and 20, as well as references therein).

In a system where superconductivity is associated with the electron-phonon coupling, the transition temperature T_c can be calculated making use of McMillan's solution of the Eliashberg equation[32]

$$T_c = \frac{\hbar \omega_{\ln}}{1.2 k_B} \exp\left[-\frac{1.04(1+\lambda)}{\lambda - \mu^*(1+0.62\lambda)} \right], \tag{5}$$

where $\omega_{\ln}$ is a typical (logarithmic averaged) phonon frequency, and μ^* the Coulomb pseudopotential.[33] While the above expression leads to $T_c \approx$ 10–15 K for C_{60}, making use of typical values $\mu^* = 0.2$–0.3, it predicts a vanishing value for C_{70}, even allowing for uncertainties of the order of 50 to 100% in the estimated value of λ.

This result testifies to the fact that the transport properties in fullerites are not simply dictated by the general features common to all these systems. Going from C_{60} to C_{70}, deformation plays a very important role with respect to the electron-phonon interaction, by breaking the symmetries of electronic and vibrational levels, and by weakening their coupling.

Similar effects have been found in the case of spherical and quadrupole deformed nuclei, in particular in connection with the effective mass,[35] but also in the case of the pairing gap,[36] and can be connected with the fact that a large fraction of the collectivity of the system becomes tight up to the static deformation of the mean field. To better understand the origin of the large reduction of the coupling strength in going from C_{60} to C_{70}, we have analyzed, for both clusters, the phonon eigenvectors of the low-frequency modes which couple to the electronic LUMO state, and compared them with the spatial localization of the latter.

In the low-frequency region, as illustrated in Ref. 18, it is possible to recognize, with no ambiguity, the relation between a group of slightly splitted vibrational modes of C_{70} and the corresponding quintuplet of an H_g mode of C_{60}. This can be done by classifying the modes of both clusters according to the largest common symmetry subgroup, C_{5v}. We focus on the $H_g(2)$ mode of C_{60} at 408 cm^{-1}, which is associated with one of the largest λ_ν. Following Ref. 18, we can trace the five modes associated with the $H_g(2)$ vibration of C_{60} to the A_1',E_1'' and E_2' modes of C_{70} at 425, 415, and 442 cm^{-1}, respectively. The E_1'' mode does not couple with the LUMO of C_{70}, hence about 2/5 of the coupling strength is lost. The remaining modes are associated with a higher $\hbar\omega$ with respect to the case of C_{60}, further reducing the coupling. Finally, a large reduction effect comes from the different spatial localization of the LUMO wave functions in C_{60} and C_{70}. In particular, we have explicitly verified that the shape of the molecular deformation associated with the above mentioned normal modes is quite similar in the two clusters.[34] However, in the case of C_{60} the LUMO wave function is concentrated in the neighborhood of the bonds which undergo the largest stretching while in C_{70}, the LUMO wave function is distributed on a larger region. We show in Fig. 1 the stereographic projection of C_{60} LUMO wave function on a spherical surface with radius 3.4 Å, while in Fig. 2 a similar projection—but on an ellipsoidal surface whose radii are 3.55, and 4.20 Å—is presented for the case of the LUMO wave function of C_{70}. In both figures, the thick continous lines mark the bonds which vary by more than 6% under the phonon displacement fields.

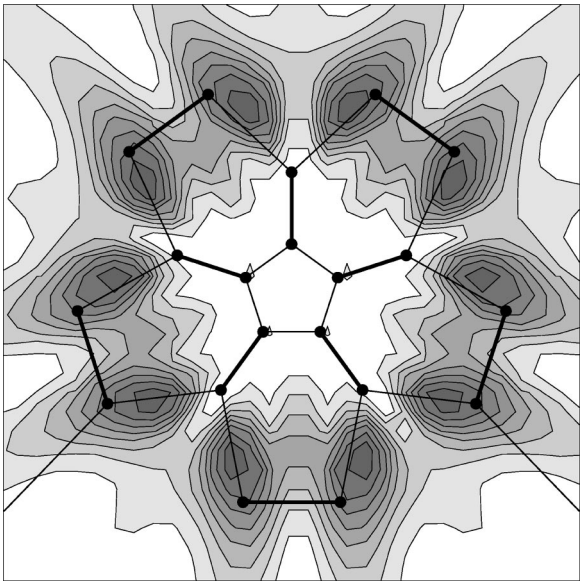

FIG. 1. Stereographic projection on a plane of the values taken by the squared C_{60} LUMO wave function on a spherical surface of radius 3.4 Å. The thick lines mark the bonds that vary more than 6% by effect of the displacement field associated with the H_g phonon at 408 cm^{-1}.

III. PHOTOEMISSION SPECTRA

The weakness of the electron-phonon matrix elements in the case of C_{70} reflects itself also in the shape of the photoemission spectrum of C_{70}^-, as is shown below. In the photoemission experiment, we are dealing with the process C_{70}^-

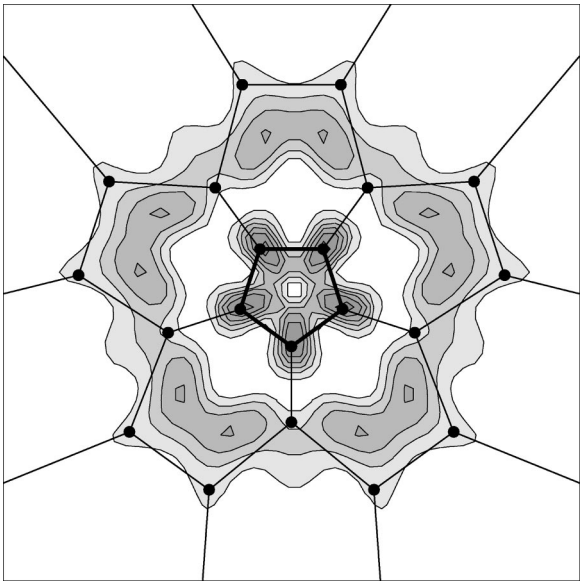

FIG. 2. Stereographic projection on a plane of the values taken by the squared C_{70} LUMO wave function on an ellipsoidal surface of radii 3.55 and 4.20 Å. The thick lines mark the bonds that vary more than 6% by effect of the displacement field associated with the A_1' phonon at 425 cm^{-1}.

$+h\nu \rightarrow C_{70}+e^-$, where $h\nu$ is the incident photon and e^- the emitted electron.

In order to define the ground state of C_{70}^-, we start from the full electron-phonon Hamiltonian,

$$H=\sum_i \varepsilon_i c_i^\dagger c_i+\sum_\alpha \hbar\omega_\alpha \Gamma_\alpha^\dagger \Gamma_\alpha + \sum_{i,j;\alpha} [V_{def}^{(\alpha)}]_{ij} c_i^\dagger c_j (\Gamma_\alpha^\dagger+\Gamma_\alpha), \tag{6}$$

where the first term contains the Kohn-Sham energies ε_i, the second term is the free phonon term, and the last term is the usual bilinear electron-phonon coupling term. The 280 valence electrons of C_{70} are assumed to be frozen (we call ψ_C their wave function), while the extra electron of C_{70}^- is assumed to occupy one of the two (degenerate) lowest unoccupied states of C_{70} whose wave functions are labeled by $\psi_i (i=1,2)$. The basis used for solving Eq. (6) is built up with these one-electron states coupled to 1, 2, or 3 different phonons (let us call ϕ_α a phonon wave function). The matrix thus obtained, which turns out to be of the order of 5000 $\times$5000, is diagonalized by using the Lanczos method. We denote by E_0 its lowest eigenvalue and by Ψ_0 the corresponding wave function. This should then describe the ground state of the charged molecule C_{70}^-,

$$\Psi_0=\sum_i a_i \psi_i \psi_C+\sum_{i,\alpha} b_i(\alpha)\psi_i\psi_C\phi_\alpha + \sum_{i,\alpha,\alpha'} c_i(\alpha,\alpha')\psi_i\psi_C\phi_\alpha\phi_{\alpha'}+\cdots. \tag{7}$$

Assuming that the emitted electron does not interact with the system left behind (sudden approximation[37]), and that its wave function is described by a plane wave, the transition probability for the emission process, from the initial state Ψ_0 to a final state of energy E_f in which the neutral C_{70} has 1, 2, or 3 phonons α excited (we denote by Φ_f the corresponding total vibrational wave function), is given by the Fermi golden rule,

$$W\sim\sum_f |\langle e^{-i\vec{k}\cdot\vec{r}}\psi_C\Phi_f|V_{ext}|\Psi_0\rangle|^2\delta(h\nu+E_0-E_f-\varepsilon), \tag{8}$$

where V_{ext} is the (dipole) external field, $E_f=\Sigma_\alpha \hbar\omega_\alpha$ (the energy of the 280 frozen electrons does not appear neither in the initial nor in the final state), and ε is the electron energy. If we substitute Eq. (7) into Eq. (8), and assume that the dominant terms are those corresponding to the LUMO (i.e., to the state ψ_1), we can factor out the dipole matrix element, and we are left with

$$W_0\sim|a_1|^2\delta(h\nu+E_0-\varepsilon) + \sum_\alpha |b_1(\alpha)|^2\delta(h\nu+E_0-\hbar\omega_\alpha-\varepsilon) + \sum_{\alpha,\alpha'} |c_1(\alpha,\alpha')|^2\delta(h\nu+E_0-\hbar\omega_\alpha-\hbar\omega_{\alpha'}-\varepsilon). \tag{9}$$

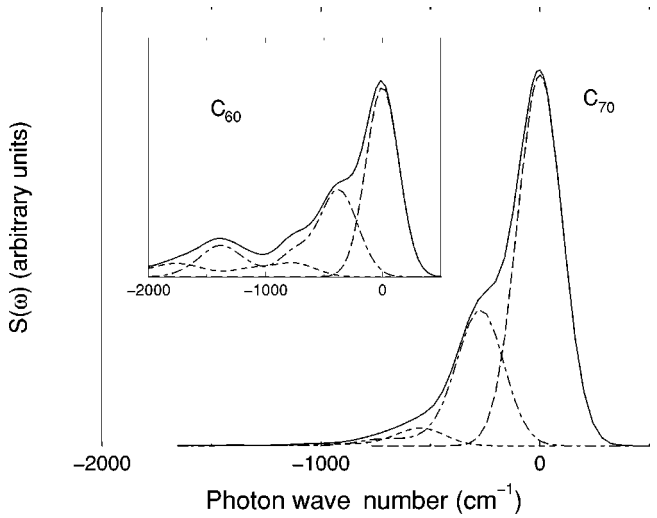

FIG. 3. Calculated photoemission spectrum for C_{70}^- (solid line). In the inset, the photoemission spectrum for C_{60}^- from Ref. 20 is shown. The contributions coming from zero phonons (long-dashed line), one phonon (dash-dotted line) and two phonons (dashed line) are also plotted separately. See the text for a discussion. A broadening with Gaussians of 40-meV width has been used in constructing the photoemission spectra.

We have plotted the results for W_0 in Fig. 3. The scale has been set in such a way that $h\nu+E_0\equiv 0$ and the numbers in the horizontal axis correspond to ε. While the shoulder at 300 cm^{-1} and the tail extending from 400 to 800 cm^{-1} indicate the presence of satellite peaks containing 1 and 2 phonons (as emphasized by the thin curves), the rather smooth behavior of the cross section and the strength of the main peak with respect to the satellites, as compared to the corresponding quantities in the case of C_{60}, testify to the fact that the electron-phonon coupling in C_{70}^- is much weaker than in C_{60}^- (see inset of Fig. 3). While the overall behavior of the photoemission cross section predicted by theory is confirmed by the experimental data, lack of resolution does not allow for a detailed comparison.

IV. CONCLUSIONS

The calculated electron-phonon coupling in C_{70} is found to be about one order of magnitude weaker than in C_{60}. In particular, we estimate the total dimensionless electron-phonon coupling constant λ to be about 0.1. The decrease with respect to C_{60} is understood on the basis of the symmetry reduction, and the different shape and spatial localization of the LUMO wave function in C_{70}. The calculated λ value is consistent with the lack of the superconducting phase transition reported in the literature at temperatures as low as 1 K. This value agrees also with the overall features of two relevant experimental measurements: the broadening of Raman peaks in K_4C_{70} and the photoemission cross section in C_{70}^-. In the latter case, experiments with higher resolution would be required to test in detail the theoretical predictions.

ACKNOWLEDGMENTS

This work has been partially supported by the INFM advanced research program CLASS.

[1] R.M. Fleming, A.P. Ramirez, M.J. Rossemsky, D.W. Murphy, R.C. Haddon, S.M. Zahmak, and A.V. Makhija, Nature (London) **352**, 788 (1991).
[2] A.F. Hebard, M.J. Rossemsky, R.C. Haddon, D.W. Murphy, S.H. Glarum, T.T.M. Palstra, A.P. Ramirez, and A.R. Kortan, Nature (London) **350**, 600 (1991).
[3] K. Hokzer, O. Klein, S.M. Huang, K.B. Kaner, K.J. Fu, R.L. Whetten, and F. Diedrich, Science **252**, 1154 (1991).
[4] M.J. Rossemsky, A.P. Ramirez, S.H. Glarum, D.W. Murphy, R.C. Haddon, A.F. Hebard, T.T.M. Palstra, A.R. Kortan, S.M. Zahmak, and A.V. Makhija, Phys. Rev. Lett. **66**, 2830 (1991).
[5] K. Tanigaki, T.W. Ebbesen, S. Saito, J. Mizuki, J.S. Tsai, Y. Kubo, and S. Kuroshima, Nature (London) **352**, 222 (1991).
[6] T.T.M. Palstra, A.F. Hebard, R.C. Haddon, and P.B. Littlewood, Phys. Rev. B **50**, 3462 (1994).
[7] J. Winter and H. Kuzmany, Phys. Rev. B **53**, 655 (1996).
[8] O. Gunnarson, Rev. Mod. Phys. **69**, 575 (1997).
[9] Z.H. Wang, K. Ichimura, M.S. Dresselhaus, G. Dresselhaus, W.-T. Lee, K.A. Wang, and P.C. Eklund, Phys. Rev. B **48**, 10 657 (1993).
[10] M. Côté, J.C. Grossmann, M.L. Cohen, and S.G. Louie, Phys. Rev. Lett. **81**, 697 (1998).
[11] A. Devos and M. Lannoo, Phys. Rev. B **58**, 8236 (1998).
[12] F. Barranco, R.A. Broglia, G. Gori, E. Vigezzi, P.F. Bortignon, and J. Terasaki, Phys. Rev. Lett. **83**, 2147 (1999).
[13] R.F. Curl and R.E. Smalley, Science **242**, 1017 (1988).
[14] W. Krätschmer, L.D. Lamb, K. Fostiropoulos, and D.R. Huffman, Nature (London) **347**, 354 (1990).
[15] N.H. Tea, R.C. Yu, M.B. Salamon, D.C. Lorents, R. Malhotra, and R.S Rouff, Appl. Phys. A: Solids Surf. **56**, 21 (1993).
[16] W. Andreoni, F. Gygi, and M. Parrinello, Chem. Phys. Lett. **189**, 241 (1992).
[17] A.K. Abdul-Sada, R. Taylor, J.P. Hare, and H.W. Kroto, J. Chem. Soc. Chem. Commun. **20**, 1423 (1990); J.R. Salem, R.D. Johnson, G. Meijer, and D.S. Bethune, J. Am. Chem. Soc. **113**, 3619 (1991).
[18] G. Onida, W. Andreoni, J. Kohanoff, and M. Parrinello, Chem. Phys. Lett. **219**, 1 (1994).
[19] G. Benedek, G. Onida, M. Righetti, and S. Sanguinetti, Nuovo Cimento D **15**, 565 (1993); S. Sanguinetti, G. Benedek, M. Righetti, and G. Onida, Phys. Rev. B **50**, 6743 (1996); **53**, 8789 (1996).
[20] N. Breda, R.A. Broglia, G. Colò, H.E. Roman, F. Alasia, G. Onida, V. Ponomarev, and E. Vigezzi, Chem. Phys. Lett. **286**, 350 (1998).
[21] J.P. Perdew and A. Zunger, Phys. Rev. B **23**, 5042 (1981).
[22] D.M. Ceperley and B.J. Alder, Phys. Rev. Lett. **45**, 566 (1980).
[23] X.J. Kong, C.T. Chan, K.M. Ho, and Y.Y. Ye, Phys. Rev. B **42**, 9357 (1990); K. Kobayashi, N. Kurita, H. Kumahora, K. Tago, and K. Ozawa, *ibid.* **45**, 13 690 (1992).
[24] G. Bachelet, D.R. Hamann, and M. Schlüter, Phys. Rev. B **26**, 4199 (1982).
[25] F. Alasia, R.A. Broglia, G. Colò, and H.E. Roman, Chem. Phys. Lett. **247**, 502 (1995).
[26] S. Saito and A. Oshiyama, Phys. Rev. B **44**, 11 532 (1991).
[27] We used the model of Ref. 19 with the following set of parameters (original values in parenthesis): $Y^2/\epsilon = 1.63(1.628)$, $\rho = 0.43(0.431)$ Å, $c = 0.36(0.511)$ Å^{-1}, $\beta = 48.7(50.5) \times 10^4$ dyn/cm and $\Phi_0 = 28.86(28.86) \times 10^{-12}$ erg. The slight differences with respect to the original values are due to the use of an improved set of equilibrium coordinates. The change in the value of c has a little effect on the BCM calculation, as can be understood from its definition in Ref. 19.
[28] As should be evident from the above discussion, g_α includes the factor $\sqrt{\hbar/2m\omega}$ coming from the matrix element of $\vec{Q}_N$ between zero- and one-phonon vibrational states (in the literaure, other definitions of g_α are sometimes found).
[29] Z.H. Wang, M.S. Dresselhaus, G. Dresselhaus, and P.C. Eklund, Phys. Rev. B **48**, 16 881 (1993).
[30] P.H.M. van Loosdrecht, M.A. Verheijen, H. Meekes, P.J.M. van Bentum, and G. Meijer, Phys. Rev. B **47**, 7610 (1993).
[31] As an example, let us consider the low-energy peak measured at 256 cm^{-1} in Ref. 29, which in Refs. 30 and 19 is resolved into two distinct modes.
[32] W.L. McMillan, Phys. Rev. **167**, 331 (1968).
[33] M. Schlüter, M. Lannoo, M. Needels, G.A. Baraff, and D. Tománek, J. Phys. Chem. Solids **53**, 1473 (1992).
[34] We have also verified that this conclusion does not depend on the model chosen to calculate the phonons: for the modes at hand, the displacement fields extracted from Car-Parrinello molecular dynamics (Ref. 18) coincide with those of BCM within a few percent.
[35] P. Donati, T. Døssing, Y.R. Shimizu, S. Mizutori, P.F. Bortingmon, and R.A. Broghu (to be published).
[36] For example, the pairing gap of the Sm-isotopes shows a clear dependence with the mass numbers correlated with the phase transition taking place from spherical to deformed shapes at mass number $A = 150$.
[37] L. Hedin and S. Lundqvist, Solid State Phys. **23**, 1 (1969).